RSC Advances

PAPER

View Article Online
View Journal | View Issue

Cite this: *RSC Adv.*, 2020, **10**, 27532

Few-layer and large flake size borophene: preparation with solvothermal-assisted liquid phase exfoliation†

Feng Zhang,[abc] Liaona She,[abc] Congying Jia,[abc] Xuexia He,[bc] Qi Li,[bc] Jie Sun,[bc] Zhibin Lei[abc] and Zong-Huai Liu*[abc]

Received 19th April 2020
Accepted 4th July 2020

DOI: 10.1039/d0ra03492d

rsc.li/rsc-advances

The preparation of two-dimensional boron (B) nanosheets, especially for borophene, is still a challenge because of its unique structure and complex B–B bonds in bulk boron. In the present work, a novel preparation technology for borophene with only a few layers and large flake sizes is developed by a solvothermal-assisted liquid phase exfoliation process, consisting of ball milling-thinning, solvothermal swelling, and probe ultrasonic delamination. The exfoliation effect of the bulk B precursors is related to the surface tension and Hildebrand parameter of the selected solvents such as acetone, *N*,*N*-dimethyl formamide (DMF), acetonitrile, ethanol, and *N*-methyl pyrrolidone (NMP), and a relative small surface tension when using solvents is favorable for the exfoliation of bulk B. Four-layer thick borophene and an average lateral size of 5.05 μm can be obtained in acetone as the exfoliating solvent. The surface composition of the exfoliated few-layer borophene with large flake size hardly changes, while the chemical state of B changes to some extent because they are partly oxidized on the surface by contaminates before and after exfoliation. This acetone solvothermal-assisted liquid phase exfoliation technique can be used to prepare high quality borophene with large horizontal sizes, and it will provide the basis to study few-layer borophene with large sizes further.

Introduction

Two-dimensional layered materials (2DMs) have an infinite crystalline structure and are made of periodic units in the plane dimensions while the atomic thickness is in the third out-of-plane dimension.[1] Because of their novel structures, 2DMs show unique electronic and optical properties from the bulk to the monolayer structure, and the reports on their preparation methods, structures, and physical electrochemical properties have gained broad interest.[2–4] From the discovery of graphene in 2004,[5] many 2DMs with novel properties and structures have been investigated, and their excellent potential applications in optoelectronics, electronics, energy conversion and storage, sensing, flexible devices, and many other fields have also been investigated.[6–11] Although many 2DMs have been designed and prepared and their structures and properties have been researched, 2DMs with novel structures and properties are still pursued in basic to applied research.

Recently, 2DMs constructed by light elements and non-metals such as boron (B), nitrogen (N), oxygen (O), and carbon (C) atoms have gained wide attention because of their diverse structures and properties.[12–15] Borophene is one form of the new 2DMs constructed by light elements and non-metals;[16] it is generally composed of single atom thick boron, and has aroused great research interest in recent years because of its tunable gap,[17] high chemical stability,[18] high energy storage capacity,[19] superconductivity,[20] and high carrier mobility.[21] However, it is distinct from carbon materials that generally have a layered structure. There are few experimental studies on borophene because the complicated structure and electron deficient characteristics of bulk boron introduce many difficulties into the borophene preparation, although several theoretical calculations indicate that layered borophene exists in a stable form.[22–25]

In order to investigate the structure and properties of borophene, pure 2D borophene must be prepared, and particularly borophene nanosheets because of their metallic nature among other elemental 2D materials.[26] In general, top-down and bottom-up methods are used to prepare 2DMs with novel structures and properties.[27] Up to now, top-down approaches, such as chemical exfoliation and sonication assisted liquid-phase exfoliation, have been widely used to prepare 2DM nanosheets from their bulk precursors.[28–31] To realize liquid-phase exfoliation of layered 2DMs, bulk layered precursors

[a]*Key Laboratory of Applied Surface and Colloid Chemistry, Shaanxi Normal University, Ministry of Education, Xi'an, 710062, P. R. China*
[b]*Shaanxi Key Laboratory for Advanced Energy Devices, Xi'an, 710119, P. R. China*
[c]*School of Materials Science and Engineering, Shaanxi Normal University, Xi'an, 710119, P. R. China. E-mail: zhliu@snnu.edu.cn*

† Electronic supplementary information (ESI) available. See DOI: 10.1039/d0ra03492d

with high quality and good crystallinity are usually required. The bulk boron layered precursor exhibits complex and diverse bulk structures and weak crystallinity due to the rich bonding configurations among B atoms, and it is very different from bulk black phosphorus, graphene, and others with naturally layered structures,[32] thus making it highly challenging to prepare borophene nanosheets with only a few layers and large sizes by direct liquid phase exfoliation methods. Thus, only a few studies have reported the preparation of few-layer borophene nanosheets by liquid phase exfoliation from B layered precursors. A few boron nanosheets with an average thickness of 1.8 nm are obtained by sonication-assisted liquid phase exfoliation of a 2D boron precursor, but their horizontal size is only a few hundred nanometers.[26] Using sonication-assisted liquid-phase exfoliation of bulk B, high-quality few-layer B sheets were prepared in large quantities by the Teo group, and the exfoliating solvent types and centrifugation speeds controlled the lateral size and thickness of the exfoliated B sheets.[33] Recently, the Vinu group investigated the exfoliation behavior of a bulk boron precursor using a sonochemical exfoliation of boron powder in various solvents; they found that acetone is an excellent exfoliation solvent, in which the obtained few-layer boron sheets have lateral dimensions as large as 1.2 μm and varying thickness from 2 nm to 18 nm (1–10 thick).[34] From the above cited work, it can be seen that although some interesting experimental results for borophene with a few layers have been obtained, the relatively thick layers and smaller size with poor uniformity do not still meet the requirements of borophene nanosheets with few layers and large size. Therefore, developing a facile and efficient method to realize homogeneous monolayer or few-layer boron nanosheets with large horizontal sizes as well as thin thickness is a challenging task.

Herein, an acetone solvothermal-assisted liquid phase exfoliation technique was developed to prepare high quality borophene with large horizontal sizes. Using the swelling effect of the acetone, the B powder precursor was first wetted in acetone. Then, the wetted B precursor was further solvothermally treated in acetone at 200 °C, followed by sonication with a probe-type sonicator at 225 W for 4 h. Borophene with a few layers of boron and a horizontal size up to 5.05 μm was finally obtained. The acetone solvothermal-assisted liquid phase exfoliation technique can be used to prepare boron nanosheets with large horizontal sizes and high quality, which can be used in basic materials research to examine borophene more critically.

Results and discussion

An acetone solvothermal-assisted liquid phase exfoliation process, which consists of ball milling-thinning, solvothermal swelling, and probe ultrasonic delamination, for bulk B precursors with layered structures is shown in Fig. 1. First, bulk B precursors were ground in acetone and thinned in a mortar for 60 min due to the relatively small surface tension of acetone among organic solvents, and a transparent dispersion was obtained. Next, the B precursor dispersion was transferred into a Teflon-lined autoclave and solvothermally treated at 200 °C for 24 h, the B precursors were further swelled from acetone

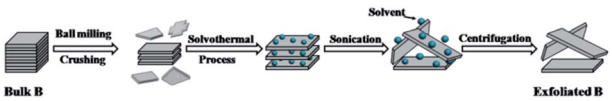

Fig. 1 Schematic illustration of borophene with few layers exfoliated by the probe ultrasonic assisted solvothermal treatment process.

molecules intercalating into the interlayer of B layers, and the weakened interlayer forces made it easier to exfoliate. Third, the transparent dispersion was sonicated with a probe-type sonicator at 225 W for 4 h, exfoliating the B precursors into few-layer borophene nanosheets suspended in acetone, similar to a black phosphorous dispersion that has been sonicated for 1 h continuously in acetonitrile.[35] The obtained cloudy dispersion was centrifuged at 6000 rpm for 20 min, the exfoliated B nanosheet supernatant was collected, and the color of the exfoliated B nanosheet supernatant was light brown compared with its original cloudy dispersion.

In order to investigate the exfoliation effect of different organic solvents with different surface tensions on bulk B precursors, dimethyl formamide (DMF), acetonitrile, ethanol, and *N*-methyl-2-pyrrolidone (NMP) were examined along with acetone. The experimental results using the same treatment condition and process are shown in Fig. 2. The SEM and TEM images of the treated B precursor dispersion in different five solvents show the exfoliation of bulk B precursors and that the sheet thickness and particle size of the obtained borophene are very different for different solvents. Although an obvious Tyndall effect for the exfoliated borophene suspension corresponding to the borophene nanosheets dispersion in solvents can be observed in five solvents (inserts of each TEM image), the exfoliation effect has obvious differences. In the five organic solvents, the exfoliation efficiency of bulk B precursors gradually decreases in the following order: acetone, DMF, acetonitrile, ethanol, and NMP, and the best exfoliation effect is

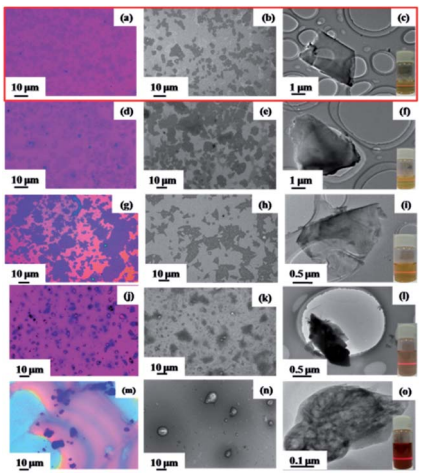

Fig. 2 Optical microscope photos, SEM images, and TEM images of borophene with few layers exfoliated in different solvents: acetone (a–c), DMF (d–f), acetonitrile (g–i), ethanol (j–l), and NMP (m–o) (the insets show the Tyndall effect of borophene dispersion with few layers).

observed in acetone. Moreover, the influence of the ultrasonic power and time on the exfoliation effect was investigated, and the experimental results are shown in Fig. S1.† It can be seen that when the ultrasonic power or reaction time increase, the morphologies of the exfoliated nanosheets differ from each other and they tend to fragment. In acetone, the obtained suspension can not only maintain good dispersibility, but also achieves the largest particle size for the obtained borophene nanosheets (Fig. 2a–c). For DMF, acetonitrile, and ethanol, the exfoliated amounts and the particle size of the obtained borophene nanosheets are intermediate for bulk B precursors (Fig. 2d–l). While in the NMP medium, the exfoliation effect is small and only partially thin and diminished boron precursors are observed in the SEM and TEM images (Fig. 2m–o). These results indicate that the exfoliated amounts and the particle size of the obtained borophene sheets are closely related to the exfoliation solvent. For acetone, DMF, acetonitrile, ethanol, and NMP, the surface tensions are 23.7, 25.7, 29.58, 22.27, and 41 mN m^{-1}, respectively,[36] suggesting that the exfoliation effect of bulk B precursors is related to the surface tension of the reaction solvents, and a solvent with a relatively small surface tension aids the exfoliation of bulk B. In addition, the Hildebrand parameter, δT, which is the square root of the ratio to total molar cohesive energy and the molar volume of the specific solvent, is commonly used for the choice of solvent in graphene exfoliation experiments according to basic solubility theory.[37,38] For acetone, DMF, acetonitrile, ethanol, and NMP, their Hildebrand parameters are 19.9, 24.9, 24.4, 26.5, and 23 $MPa^{1/2}$, respectively,[39] indicating that the good exfoliation effect of bulk B can be obtained in the solvent with a small surface energy and Hildebrand parameter. In addition, the colloidal stability of the delaminated borophene suspensions in acetone and acetonitrile was tested when they were placed at room temperature for three months. The acetone suspension exhibit the clear Tyndall effect and few obvious precipitation, indicating that it has good dispersion compared with that in other solvents (Fig. S2†).

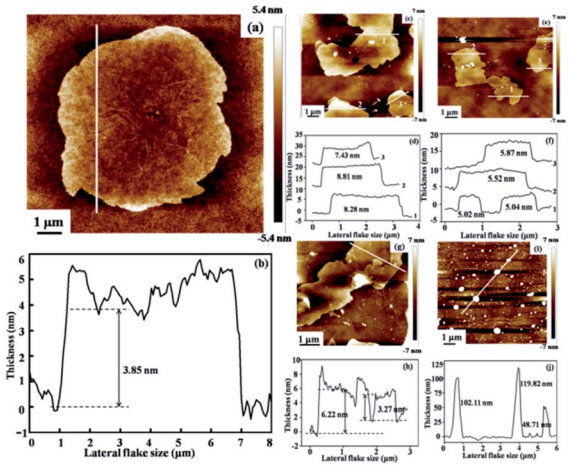

Fig. 3 AFM images and the corresponding height profiles of borophene with few layers exfoliated in different solvents: acetone (a and b), DMF (c and d), acetonitrile (e and f), ethanol (g and h), and NMP (i and j), respectively.

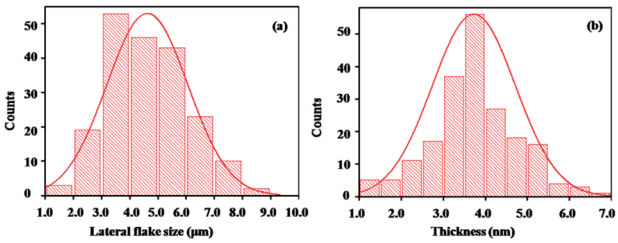

Fig. 4 Statistical data showing the lateral flake size average (a) and the thickness (b) of borophene with few layers in acetone.

In general, the ideal exfoliation for 2DM layered compounds leads to few-layer or monolayer nanosheets. Therefore, the thickness and lateral flake size of the exfoliated nanosheets in different solvents are characterized by AFM, and the experimental results are shown in Fig. 3. It can be seen that nearly homogeneous thickness is observed in acetone in different selected areas, and the average thickness is about 3.5 nm (Fig. 3a and b). Because the thickness of borophene nanosheets is about 0.8 nm,[34] the exfoliated borophene consists of four B layer nanosheets. On the other hand, either the thickness or transverse dimensions from the obtained suspensions in other solvents are not better than that of the obtained suspension in acetone, suggesting that acetone is the ideal exfoliation solvent for bulk B precursor. More importantly, the homogeneous distribution of the exfoliated borophene thickness and the small lateral flake size are displayed in the images (Fig. 3c–j). The AFM statistical results indicate that the lateral flake size and the thickness of the exfoliated borophene in acetone are 5.05 μm and 3.5 nm, respectively (Fig. 4a and b). Plots of the lateral size *vs.* thickness for the delaminated borophene nanosheets in acetone show that the average size distribution of the borophene nanosheets are between 2.35 to 6.58 μm and less than 5 nm thickness, indicating that the delaminated borophene is few-layered and has large flake sizes (Fig. S3†). On the other hand, the lateral flake size and the thickness of the exfoliated borophene in the other four solvents show an inhomogeneous distribution (Fig. S4 and S5†).

A comparison between literature results and the present finding on the size and thickness of borophene nanosheets obtained by liquid-phase exfoliation is shown in Table 1. It can be seen that the solvothermal-assisted liquid phase exfoliation provides an effective strategy for preparing borophene with large sizes and few-layers. The Vinu group reported free-standing borophene sheets obtained in various solvents, and

Table 1 The comparison between literature results and the present finding on the size and thickness of borophene with few layers by liquid-phase exfoliation

Dispersant	Thickness	Size	Reference
DMF	1.8 nm	200 nm	33
IPA	4.7 nm	<100 nm	33
Acetone	2–18 nm	1.2 μm	34
Acetone	3.5 nm	5.05 μm	Our work

acetone performed exceedingly well for the exfoliation. Although different B sheets are obtained under variable centrifugation speed and corresponding times, the largest lateral dimension of their B sheets was only 1.2 μm, which is much smaller than 5.05 μm in this work. Therefore, it is concluded that borophene with a few layers and large flake sizes can be prepared by an acetone solvothermal-assisted liquid phase exfoliation process from selected bulk B precursors. Since the best exfoliation effect of bulk B precursors was achieved in acetone, the obtained borophene was further characterized for the remainder of the report.

By freeze-drying the suspension of the exfoliated borophene in acetone, the obtained morphologies with low and high resolution are shown in Fig. 5a and b. Compared to the morphology of bulk B precursor (Fig. S6†), an obvious loose flake morphology is observed (Fig. 5a), and the parallel layered structure is clearly shown in high resolution in Fig. 5b. The formation of the parallel layered structure may be evidence for the exfoliated state of bulk B precursors, supporting the occurrence of exfoliation in acetone. The exfoliated state of 2DMs is a thermodynamically metastable state, so it only takes place under specific conditions. Therefore, the exfoliated nanosheets are usually restacked and reform the parallel layered structure during the drying process, which is confirmed by freeze-drying the suspension of exfoliated borophene. In order to thoroughly investigate its morphology and crystal structure, the exfoliated borophene was further characterized by TEM and HRTEM. The TEM image shows the thinner and larger restacked parallel layered morphology (Fig. 5c). The HRTEM image (Fig. 5d) and the corresponding fast Fourier transform (FFT) diffraction pattern of the representative (Fig. 5e) shows the clear interference fringe with a *d*-spacing of 0.504 nm, which corresponds to the (104) plane of a β-rhombohedral boron structure,[40] suggesting that the crystalline state of the exfoliated borophene in acetone does not change.

HAADF STEM and corresponding EELS elemental mapping images of the exfoliated borophene indicate that B is uniformly distributed throughout the whole nanosheet, and a certain amount of C and N are found on some edges of the nanosheet (Fig. 6). The contents of B, C and N are 55.22%, 30.40% and 0.67%, respectively, and the remaining component is probably ascribed to O. The large amounts of C are caused by a carbon

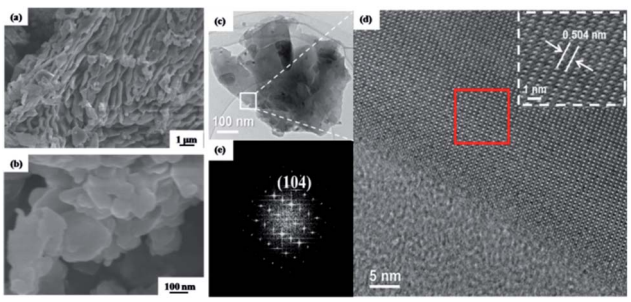

Fig. 5 SEM images with low resolution (a) and high resolution (b) and TEM images of borophene with few layers obtained by probe ultrasonic assisted solvothermal exfoliation in acetone and corresponding FFT pattern of the selected area (c–e).

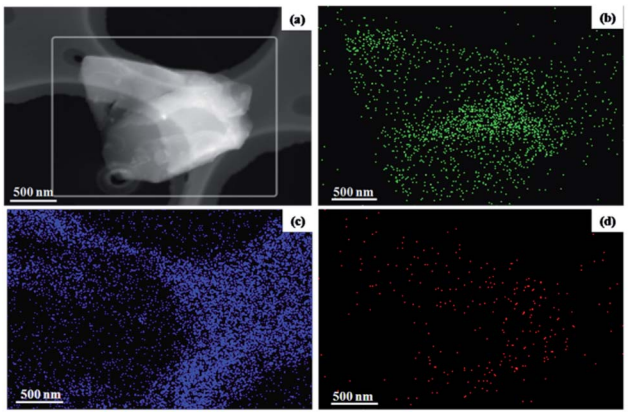

Fig. 6 HAADF STEM and corresponding EELS elemental mapping images of borophene with few layer boron sheets by probe ultrasonic assisted solvothermal exfoliation, followed by centrifugation treatment in acetone: STEM image (a), boron (b), carbon (c), and oxygen (d).

film, and the small amounts of N and O are likely due to the surface contamination that occur during exposure to an air atmosphere and the exfoliating solvent. In the following XPS characterization of the bulk B precursor, large amounts of oxygen are detected, suggesting that the small amount of O in the EELS elemental mapping image for the exfoliated borophene is mainly derived from the bulk B precursor itself.

For the exfoliated borophene, the phase purity and crystalline structure was further characterized by XRD and Raman spectroscopy, in comparison with the bulk B precursors, and the experimental results are shown in Fig. 7. Compared with the XRD pattern of the bulk B precursors, a similar XRD pattern is observed, and most of the major diffraction peaks can be indexed to the β-rhombohedral boron (JCPDF 00-031-0207), suggesting that the crystalline structure is nearly conserved before and after the exfoliation. However, minor changes in that the diffraction peak intensity decreased for the exfoliated borophene were found, suggesting that the crystals may have a preferred orientation during the exfoliation process (Fig. 7a). Raman spectroscopy is an effective method to characterize the atomic bonding in materials. Because of the anisotropy, no identical symmetry axes, and atomic displacements toward the atomic ridges of borophene, more characteristic Raman peaks for borophene should be observed. Except for the weak series of Raman peaks, the characteristic peak at 1070 cm^{-1}

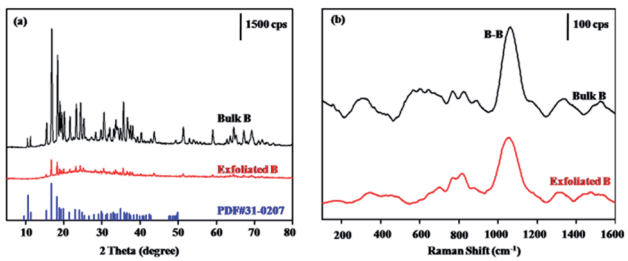

Fig. 7 XRD patterns (a) and Raman spectra (b) of bulk B and borophene with few layers obtained by probe ultrasonic assisted solvothermal exfoliation.

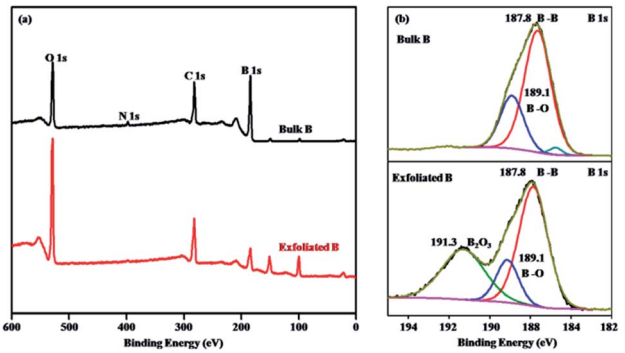

Fig. 8 XPS spectra (survey) (a) and short scan XPS B 1s (b) of bulk B and borophene with few layers obtained by probe ultrasonic assisted solvothermal exfoliation.

corresponding to the vibration mode of inter-icosahedral B–B bonds[21] is observed in both samples before and after exfoliation, suggesting that the atomic bonding hardly changes for the exfoliated borophene (Fig. 7b).

In order to investigate changes in the surface composition and chemical state of B layers before and after exfoliation, XPS was utilized. From the XPS survey scan spectra of B bulk and the exfoliated borophene ranging from 0 to 600 eV, it can be seen that the main peaks corresponding to B, C, O, and N are maintained for the two samples, and the B content does not undergo any obvious change, suggesting that their surface compositions hardly change before and after exfoliation (Fig. 8a). The quantitative evaluation of the obtained material composition for both bulk B and the exfoliated borophene is listed in Table 2, indicating that the main composition is still B and some B is oxidized during the exfoliation process. The presence of O and C in the XPS spectra primarily arises due to airborne impurities and residual solvents. However, the peak intensity corresponding to the amount of O species is sharp in comparison with that of B bulk, indicating that the chemical state of B changes to some extent, suggesting that the exfoliated borophene is probably oxidized on the surface when it is exposed to air. Therefore, the high-resolution B 1s spectra for the two samples was further analyzed. It consists of three peaks centered at 191.3, 189.1, and 187.8 eV, respectively, indicating that B formed three types of bonding structures (Fig. 8b). The main component at 187.8 eV corresponding to a B–B bond has not changed, and it is consistent with the reported value obtained from bulk B (187.3–187.9 eV).[41] The peak centered at 189.1 eV assigned to the B–O bond in a boron-rich oxide hardly changes for the exfoliated borophene compared with B bulk.

Table 2 Evaluation of atomic ratios for both bulk boron and exfoliated borophene with few layers

Element	At%/bulk	At%/exfoliation
O 1s	12.69	25.47
C 1s	22.65	25.14
N 1s	0.75	0.67
B 1s	63.91	48.72

The peak centered at 191.3 eV obviously becomes sharp due to the formation of B_2O_3 for the exfoliated borophene,[33] suggesting that the exfoliated borophene may be partly oxidized due to its large contact area in compare with B bulk.

Conclusions

An acetone solvothermal-assisted liquid phase exfoliation process was developed to prepare borophene with a few layers and large flake sizes. It consists of ball milling-thinning, solvothermal swelling, and probe ultrasonic delamination. The exfoliation effect of bulk B precursors is related to the surface tension of the used solvents, and a relatively small surface tension of solvent is favorable for the exfoliation of bulk B. Four-layer borophene and an average lateral flake size of 5.05 μm can be obtained. It is the largest size borophene with so few layers. For the exfoliated few-layer borophene with large flake size, the surface composition was conserved, while the chemical state of B changes to some extent because they are partly oxidized on the surface before and after exfoliation. This is a facile and effective method to produce few-layer borophene with large flake sizes and may be extended to other 2D materials with no analogous bulk layered allotropes.

Materials and methods

Materials

Boron powder (purity-99.5%) was purchased from Sigma Aldrich. All chemicals were of analytical grade and used without further purification.

Preparation of borophene with few-layer and large flake size

Briefly, 100 mg of boron powder was first added into 100 mL of acetone, and a homogeneous boron dispersion was formed after vigorously stirring for 2 h at room temperature. Then, the dispersion was transferred into two 100 mL Teflon autoclaves solvothermally treated at 200 °C for 24 h. After cooling naturally to room temperature, the obtained suspension was sonicated at 225 W for 4 h, with 2 s ultrasonication and 4 s pause with a probe-type sonicator. Afterward, the mixture was centrifuged at 6000 rpm for 20 min to remove unexfoliated boron particles. The supernatant was collected for further structural characterization. By changing the exfoliated solvents to DMF, NMP, acetonitrile and ethanol, the exfoliation behavior of bulk B precursors in these solvents was also studied by a similar process.

Characterization

The morphology of bulk boron powder and the exfoliated borophene were characterized by scanning electron microscopy (SEM, TM-3000), field-emission scanning electron microscopy (FESEM, SU8020), and transmission electron microscopy (TEM, JEM 2100). The thickness and size of the exfoliated borophene were measured with atomic force microscopy (AFM, Dimension FastScan). The composition and chemical state were determined by XPS (PHI Quantera II) and the binding energy

calibration was referenced to C 1s at 284.8 eV. The X-ray diffraction (XRD) patterns were collected using a D/Max-3c X-ray diffractometer with Cu Kα radiation ($\lambda = 1.5406$ Å), scanning from 5° to 80° and using an operating voltage and current of 40 kV and 15 mA. Raman spectra were measured and collected using a Renishaw inVia with an excitation wavelength of 532 nm. AFM samples were prepared by dropping the exfoliated borophene dispersion onto a Si substrate followed by drying naturally or under vacuum at 50 °C for several hours. TEM samples were prepared by directly dropping the exfoliated borophene dispersion onto holey carbon TEM grids (Cu, 400 mesh) followed by drying naturally. SEM samples were prepared the same as the AFM samples or using freeze-dried powder of the exfoliated borophene dispersion directly.

Conflicts of interest

There are no conflicts to declare.

Acknowledgements

This work was financially supported by the National Natural Science Foundation of China (21471093, 51772182), the 111 Project, the Fundamental Research Funds for the Central Universities (GK201801010, GK201903050).

References

1 C. N. R. Rao, H. S. S. Ramakrishna Matte and U. Maitra, *Angew. Chem., Int. Ed.*, 2013, **52**, 13162.
2 Y. Wang, N. Xu, D. Li and J. Zhu, *Adv. Funct. Mater.*, 2017, **27**, 1604134.
3 C. Tan, Z. Lai and H. Zhang, *Adv. Mater.*, 2017, **29**, 1701392.
4 X. Liu, T. Ma, N. Pinna and J. Zhang, *Adv. Funct. Mater.*, 2017, **27**, 1702168.
5 K. S. Novoselov, A. K. Geim, S. V. Morozov, D. Jiang, Y. Zhang, S. V. Dubonos, I. V. Grigorieva and A. A. Firsov, *Science*, 2004, **306**, 666.
6 J. Li, X. Guan, C. Wang, H. C. Cheng, R. Ai, K. Yao, P. Chen, Z. Zhang, X. Duan and X. Duan, *Small*, 2017, **13**, 1701034.
7 J. Dong, F. Liu, F. Wang, J. Wang, M. Li, Y. Wen, L. Wang, G. Wang, J. He and C. Jiang, *Nanoscale*, 2017, **9**, 7519.
8 H. J. Choi, S. M. Jung, J. M. Seo, D. W. Chang, L. Dai and J.-B. Baek, *Nano Energy*, 2012, **1**, 534.
9 X. Tang, A. Du and L. Kou, *Wiley Interdiscip. Rev.: Comput. Mol. Sci.*, 2018, **8**, e1361.
10 L. Gao, *Small*, 2017, **13**, 1603994.
11 A. Kumar and Q. Xu, *ChemNanoMat*, 2018, **4**, 28.
12 N. R. Glavin, R. Rao, V. Varshney, E. Bianco, A. Apte, A. Roy, E. Ringe and P. M. Ajayan, *Adv. Mater.*, 2020, **32**, 1904302.
13 B. Akuzum, K. Maleski, B. Anasori, P. Lelyukh, N. J. Alvarez, E. C. Kumbur and Y. Gogotsi, *ACS Nano*, 2018, **12**, 2685.
14 F. Bu, M. M. Zagho, Y. Ibrahim, B. Ma, A. Elzatahry and D. Zhao, *Nano Today*, 2020, **30**, 100803.
15 G. Gu, M. Schmid, P. W. Chiu, A. Minett, J. Fraysse, G. T. Kim, S. Roth, M. Kozlov, E. Muñoz and R. H. Baughman, *Nat. Mater.*, 2003, **2**, 316.
16 Z. Zhang, Y. Yang, G. Gao and B. I. Yakobson, *Angew. Chem., Int. Ed.*, 2015, **54**, 13022.
17 T. Ogitsu, E. Schwegler and G. Galli, *Chem. Rev.*, 2013, **113**, 3425.
18 Z. Q. Wang, T. Y. Lü, H. Q. Wang, Y. P. Feng and J. C. Zheng, *Front. Phys.*, 2019, **14**, 33403.
19 X. Zhang, J. Hu, Y. Cheng, H. Y. Yang, Y. Yao and S. A. Yang, *Nanoscale*, 2016, **8**, 15340.
20 B. Peng, H. Zhang, H. Shao, Z. Ning, Y. Xu, G. Ni, H. Lu, D. W. Zhang and H. Zhu, *Mater. Res. Lett.*, 2017, **5**, 399.
21 J. Xu, Y. Chang, L. Gan, Y. Ma and T. Zhai, *Adv. Sci.*, 2015, **2**, 1500023.
22 L. Peng, Z. Xu, Z. Liu, Y. Wei, H. Sun, Z. Li, X. Zhao and C. Gao, *Nat. Commun.*, 2015, **6**, 5716.
23 D. L. V. K. Prasad and E. D. Jemmis, *Phys. Rev. Lett.*, 2008, **100**, 165504.
24 X. Yang, Y. Ding and J. Ni, *Phys. Rev. B: Condens. Matter Mater. Phys.*, 2008, **77**, 041402.
25 K. C. Lau, R. Pati, R. Pandey and A. C. Pineda, *Chem. Phys. Lett.*, 2006, **418**, 549.
26 S. Y. Xie, Y. Wang and X.-B. Li, *Adv. Mater.*, 2019, **31**, 1900392.
27 S. Das, M. K. Bera, S. Tong, B. Narayanan, G. Kamath, A. Mane, A. P. Paulikas, M. R. Antonio, S. K. R. S. Sankaranarayanan and A. K. Roelofs, *Sci. Rep.*, 2016, **6**, 28195.
28 M. Yi and Z. Shen, *J. Mater. Chem. A*, 2015, **3**, 11700.
29 C. Gibaja, D. Rodriguez-San-Miguel, P. Ares, J. Gómez-Herrero, M. Varela, R. Gillen, J. Maultzsch, F. Hauke, A. Hirsch, G. Abellán and F. Zamora, *Angew. Chem., Int. Ed.*, 2016, **55**, 14345.
30 H. Nakano, T. Mitsuoka, M. Harada, K. Horibuchi, H. Nozaki, N. Takahashi, T. Nonaka, Y. Seno and H. Nakamura, *Angew. Chem., Int. Ed.*, 2006, **118**, 6451.
31 Z. Xie, C. Xing, W. Huang, T. Fan, Z. Li, J. Zhao, Y. Xiang, Z. Guo, J. Li, Z. Yang, B. Dong, J. Qu, D. Fan and H. Zhang, *Adv. Funct. Mater.*, 2018, **28**, 175833.
32 V. Nicolosi, M. Chhowalla, M. G. Kanatzidis, M. S. Strano and J. N. Coleman, *Science*, 2013, **340**, 1226419.
33 H. Li, L. Jing, W. Liu, J. Lin, R. Y. Tay, S. H. Tsang and E. H. T. Teo, *ACS Nano*, 2018, **12**, 1262.
34 P. Ranjan, T. K. Sahu, R. Bhushan, S. S. Yamijala, D. J. Late, P. Kumar and A. Vinu, *Adv. Mater.*, 2019, **31**, 1900353.
35 Z. Yan, X. He, L. She, J. Sun, R. Jiang, H. Xu, F. Shi, Z. Lei and Z.-H. Liu, *J. Materiomics*, 2018, **4**, 129.
36 G. M. Forker, *Adv. Manuf. Process.*, 1957, **83**, 687.
37 Y. Hernandez, M. Lotya, D. Rickard, S. D. Bergin and J. N. Coleman, *Langmuir*, 2010, **26**, 3208.
38 A. O'Neill, U. Khan, P. N. Nirmalraj, J. Boland and J. N. Coleman, *J. Phys. Chem. C*, 2011, **115**, 5422.
39 C. Hansen, *Hansen Solubility Parameters: A User's Handbook*, 2nd edn, 2012.
40 J. J. Ipus, J. S. Blázquez, S. Lozano-Perez and A. Conde, *Philos. Mag.*, 2009, **89**, 1415.
41 T. T. Xu, J. G. Zheng, N. Q. Wu, A. W. Nicholls, J. R. Roth, D. A. Dikin and R. S. Ruoff, *Nano Lett.*, 2004, **4**(5), 963.